

# Mechanics of Force Propagation in TonB-Dependent Outer Membrane Transport

James Gumbart,\* Michael C. Wiener,<sup>†</sup> and Emad Tajkhorshid<sup>‡</sup>

\*Department of Physics and Beckman Institute, and <sup>‡</sup>Department of Biochemistry and Beckman Institute, University of Illinois at Urbana-Champaign, Urbana, Illinois; and <sup>†</sup>Department of Molecular Physiology and Biological Physics, University of Virginia, Charlottesville, Virginia

**ABSTRACT** For the uptake of scarce yet essential organometallic compounds, outer membrane transporters of Gram-negative bacteria work in concert with an energy-generating inner membrane complex, thus spanning the periplasmic space to drive active transport. Here, we examine the interaction of TonB, an inner membrane protein, with an outer membrane transporter based upon a recent crystal structure of a TonB-transporter complex to characterize two largely unknown steps of the transport cycle: how energy is transmitted from TonB to the transporter and how energy transduction initiates transport. Simulations of TonB in complex with BtuB reveal that force applied to TonB is transmitted to BtuB without disruption of the very small connection between the two, supporting a mechanical mode of coupling. Based on the results of different pulling simulations, we propose that the force transduction instigates a partial unfolding of the pore-occluding luminal domain of the transporter, a potential step in the transport cycle. Furthermore, analysis of the electrostatic potentials and salt bridge interactions between the two proteins during the simulations hints at involvement of electrostatic forces in long-range interaction and binding of TonB and BtuB.

## INTRODUCTION

The uptake of nutrients, especially those existing at extremely low concentrations, is not an easy task for Gram-negative bacteria. Although smaller molecules are free to pass through open porins in the outer membrane (OM), molecules above 600 Da must use an alternate means to enter the periplasmic space (1,2). Due to the lack of chemical energy at the OM, specialized transport systems have evolved to fill this niche. By coupling energy generated by the proton-motive force in the cytoplasmic membrane (CM) to an OM transporter, these large and scarce molecular complexes can be brought across the otherwise impermeable OM.

One such class of transporters is the TonB system. The protein TonB is anchored to the CM by a transmembrane helix where it interacts with other proteins to generate energy (3). To effect transport, it then interacts with a TonB-dependent transporter (TBDT) in the OM in an as yet unknown manner. The TBDT binds the substrate on the extracellular side, and then is somehow altered by TonB to release it into the periplasm. Specific examples of TBDTs include the iron siderophore transporter FhuA and the cobalamin (for example, vitamin B<sub>12</sub>) transporter BtuB.

A number of crystallographic structures of TBDTs, both with and without their respective substrates, have served to clarify some of the key structural elements of these systems (4–11). They are all structurally homologous, having a membrane-bound, 22-stranded  $\beta$ -barrel combined with a large N-terminal domain, the “luminal domain”, folding back into and blocking the interior of the barrel. How the

luminal domain changes conformation to allow the substrate passage was a question immediately posed by the crystal structures; suggestions put forth included some conformational change while remaining in the barrel, removal from the barrel as a singular unit, or unfolding, fully, or partially (12–14). Also, a conserved short sequence usually near the amino terminus, and identified by genetic and biochemical studies, is critical for transport function and interaction with TonB (15–19). This conserved “Ton-box” is ordered in the absence of substrate. In the presence of bound substrate however, the Ton-box undergoes an order to disorder transition and is more highly exposed to the periplasmic space, presumably as a recognition element for TonB binding (4,7,14,20,21). Based on the structures, specifically those of FhuA with and without substrate, simulations were performed to better understand the allosteric change in the TBDT that takes place when the substrate binds (22). However, at the time, it was not possible to further investigate the coupling between TonB and the TBDT since precise structural knowledge of the interactions between the two was not available.

This important yet missing piece was finally solved with the determination of two independent crystal structures of TonB in complex with two TBDTs, revealing in molecular detail their association before the energized active transport step (23,24). A structure of the *Escherichia coli* cobalamin transporter BtuB:TonB complex was solved at 2.1 Å resolution ( $R = 19.2\%$ ,  $R_f = 25.1\%$ , Protein Data Bank accession No. 2GSK) (23). Also, concurrently, a structure of the *E. coli* ferrichrome transporter FhuA:TonB complex was solved at 3.3 Å resolution ( $R = 28.4\%$ ,  $R_f = 32.9\%$ , PDB accession No. 2GRX) (24). The TBDT-interacting C-terminal domain of TonB (present in the structures of these two complexes as

Submitted January 9, 2007, and accepted for publication March 20, 2007.

Address reprint requests to Emad Tajkhorshid, Tel.: 217-244-6914; Fax: 217-244-6078; E-mail: emad@life.uiuc.edu.

Editor: Ivet Bahar.

© 2007 by the Biophysical Society

0006-3495/07/07/496/09 \$2.00

doi: 10.1529/biophysj.107.104158

well as in previously solved structures as a soluble protein domain (25–27)) forms a three-stranded  $\beta$ -sheet that is then joined by a fourth strand contributed by the Ton-box of the TBDT (23,24). While providing a detailed view of the interaction between TonB and BtuB in complex, the structures alone do not explain how this interaction leads to substrate transport. Two mechanistic models for function have been put forth. In the “shuttle” model (28,29), TonB leaves the CM entirely, crosses the periplasm in an energized form, and then imparts this energy to the transporter. Evidence for the shuttle model consists, primarily, of two types of experimental observations. First, TonB was found to be associated with both OM and CM in fractionated cells (28). Second, the periplasmic accessibility of an amino-terminal residue of TonB was characterized (29). TonB is predicted to have a single transmembrane helix, with its amino terminus in the cytosol. A residue in the amino terminus was labeled by a reagent in the periplasmic space (that does not permeate the CM into the cytosol). In the “pulling” model (14,23), it is posited that a mechanical interaction occurs, where TonB reaches across the periplasm to pull upon the luminal domain and thus open the transporter. This hypothesis (14) was initially based upon the homology between the protein fold (and orientation) of the luminal domain, and the protein fold (IgG/ubiquitin) utilized in single-molecule unfolding experiments (30,31); both are core four-stranded  $\beta$ -sheets. In experimental and computational unfolding studies, small forces exerted approximately perpendicularly to the  $\beta$ -strands of the sheet cause unfolding. A similar orientation of the luminal domain with respect to the periplasmic-facing surface of the OM suggested that TonB might apply forces of similar direction and magnitude, and thus effect a similar unfolding.

Here, we examine the pulling model by molecular dynamics (MD) simulations of TonB in complex with BtuB (see Fig. 1). MD has been successfully applied to the understanding of structure-function relationships of membrane as well as mechanically activated proteins previously (32–34). In this article, the first simulation study of the complex, we have performed  $\sim 100$  ns of steered MD (SMD) (35) to focus on two issues: the mechanism of coupling between TonB and BtuB, and the conformational changes in the luminal domain during the SMD simulations. Our results dramatically display a very strong attachment between TonB and the Ton-box of BtuB, comprised of only a few residues, that is maintained during mechanical pulling of TonB away from the OM. We also observe the luminal domain of BtuB to unfold under such a force, indicating that TonB is capable of transducing an applied force of sufficient magnitude to open a path for substrate translocation. However, we find that the force required to pull the luminal domain out of the barrel as a singular unit is 10 times higher than that required to unfold it under the same conditions. Based on the results presented here, we propose partial unfolding of the luminal domain as a key step in the mechanism of active transport in TonB-dependent outer membrane transporters.

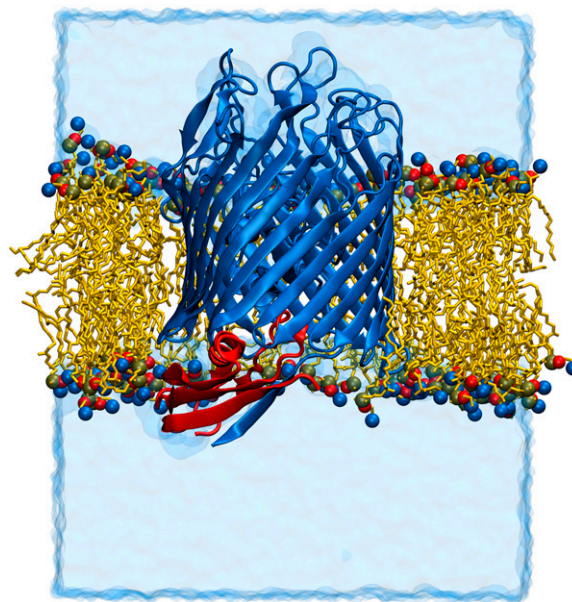


FIGURE 1 Side view of the simulated system of TonB/BtuB in a lipid/water environment. The proteins are shown in a cartoon representation with BtuB colored in blue and TonB in red. The lipids are shown in yellow with three atoms of each headgroup highlighted as spheres. The water box is drawn in a transparent blue representation. To more clearly display the protein, some lipids have been removed from the front face.

## METHODS

### Modeling

Modeling of the TonB/BtuB system began with coordinates obtained through x-ray crystallography (PDB code 2GSK) (23). All missing hydrogen atoms were placed into the structure using VMD (36). Additional molecules crystallized with the protein (calcium ions, detergent molecules, etc.) were removed, including the cyanocobalamin, which has not yet been parameterized for the CHARMM force field. Crystallographic water molecules present inside the barrel of BtuB were, however, retained.

Standard protonation states of titratable residues were chosen based on a pH of 7; approximate estimates of pKa values indicated that only a handful of residues had the potential to exist in a different state, but they did not appear to be critical in interactions of the BtuB barrel with either TonB or the luminal domain. The protein was then placed in a POPE lipid bilayer by aligning a hydrophobic band of the protein with the core of the bilayer while at the same time keeping charged residues hydrated. The protein/lipid system was solvated above and below the membrane patch with water. Sodium and chloride ions were added to 100 mM concentration in a ratio ensuring the system remained neutral (see Fig. 1).

### Molecular dynamics protocol

All molecular dynamics (MD) simulations were performed using the program NAMD 2.5 (37) and the CHARMM27 force field (38). Electrostatic interactions were evaluated using a multiple time stepping algorithm in which bonded interactions are computed every 1 fs, short-range nonbonded interactions every 2 fs, and long-range interactions (defined here as those beyond a 12-Å cutoff) every 4 fs. For long-range interactions, the particle-mesh Ewald (PME) method was used with a grid density  $>1/\text{Å}^3$ . Nearly all simulations were carried out at constant temperature (310 K) in the NVT ensemble. Constant temperature was enforced through Langevin dynamics

applied to the heavy atoms of lipids (damping coefficient of  $1 \text{ ps}^{-1}$ ) while, during equilibration, a Nose-Hoover Langevin piston was used to ensure a constant pressure. Periodic boundary conditions were employed for all simulations. The distance between protein images in neighboring periodic cells was never allowed to be  $<15 \text{ \AA}$ . A time step of  $1 \text{ fs}$  was used in all simulations.

A multistage equilibration was used to relax the system. First, all atoms except those in the lipid tails were restrained, allowing the tails to “melt”; this stage was the only one performed at constant volume and lasted  $0.5 \text{ ns}$ . A second stage freed the lipids and water completely, restraining only the protein backbone for  $1 \text{ ns}$ . Finally, everything was released for  $3.5 \text{ ns}$  of dynamics, giving a total of  $5 \text{ ns}$  for the equilibration before beginning SMD simulations. The structure proved to be stable during this time; the root mean-square deviation (RMSD) of the backbone of the individual proteins each reached a maximum value of  $\sim 1.5\text{--}2 \text{ \AA}$  as compared to the crystal structure (see supplemental Fig. S5, Supplementary Material).

## Steered molecular dynamics

For one set of simulations, those causing unfolding of the luminal domain (from here on referred to as “unfolding simulations”), steered molecular dynamics (SMD) (35,39,40) was used to pull the N-terminal  $C_{\alpha}$  atom of TonB away from the membrane and BtuB. This method is implemented, for constant velocity pulling, via a spring connecting the pulled atom with an imaginary point traveling at a constant velocity along the direction of the applied force. All simulations reported in this study began from the same equilibrated state; three simulations were conducted using velocities of  $10$ ,  $5$ , and  $2.5 \text{ \AA/ns}$ , respectively, along with a spring constant  $k = 350 \text{ pN/\AA}$ . The simulation at  $10 \text{ \AA/ns}$  lasted for  $15 \text{ ns}$  and was continued with TonB and residues  $5\text{--}39$  of BtuB removed for an additional  $13 \text{ ns}$  giving a total extension of  $280 \text{ \AA}$ . The simulation at  $5 \text{ \AA/ns}$  lasted for  $19 \text{ ns}$  and produced  $95 \text{ \AA}$  of extension, whereas the simulation at  $2.5 \text{ \AA/ns}$  lasted for  $36 \text{ ns}$  and resulted in  $85 \text{ \AA}$  of extension. Data given in the article refer to the simulation at  $2.5 \text{ \AA/ns}$ , unless stated otherwise, but key results were common to all unfolding simulations.

In addition to the unfolding simulations, we also performed a simulation in which the luminal domain was pulled out of the barrel by applying force to its center of mass. This simulation, referred to as the “unplugging simulation”, was performed with a velocity of  $2.5 \text{ \AA/ns}$  and a spring constant  $k = 350 \text{ pN/\AA}$ , identical to the slowest of the unfolding simulations. The center of mass of the luminal domain is defined here as that of the  $C_{\alpha}$  atoms of residues  $20\text{--}130$  of BtuB. TonB was removed from the system before pulling the luminal domain.

## System adjustments

To avoid too large system sizes and thus prohibitive computational effort, an adaptive procedure was developed for the unfolding simulations. For the beginning of the SMD simulation, a constant system size was used, but alterations were made to TonB directly. This required cutting the N-terminus of TonB, deleting those fully stretched residues no longer in contact with the rest of the protein. For example, in the simulation where TonB was pulled at  $2.5 \text{ \AA/ns}$ , residues Pro<sup>153</sup> to Ser<sup>156</sup> were removed at  $10.5 \text{ ns}$ . The new last residue was terminated such that it was neutral.

When this became insufficient due to the movement of the entire TonB molecule, increasing the system size became necessary. As such, an extra layer of water was added along with ions to maintain the net ionic concentration; all water was then equilibrated for  $5 \text{ ps}$  while the protein and membrane were held fixed. For the systems pulled at  $5 \text{ \AA/ns}$  and  $2.5 \text{ \AA/ns}$ ,  $60 \text{ \AA}$  of water was added, and the simulation was continued for  $12$  and  $22 \text{ ns}$ , respectively. The system size, initially  $96,000$  atoms, grew to  $145,000$  by the end of the simulation. For the system pulled at  $10 \text{ \AA/ns}$ , first  $30 \text{ \AA}$  of water was added at  $7 \text{ ns}$  and then  $60 \text{ \AA}$  at  $10 \text{ ns}$ , ending with a total of  $168,000$  atoms.

## Analysis

VMD was used for nearly all analysis and visualization. Salt bridges were defined to be present if the distance between the oxygen and nitrogen atoms of the respective residues was  $<3.2 \text{ \AA}$ ; they were considered to be stable if the average distance over equilibration was  $<4.0 \text{ \AA}$ . Sequence alignments and comparison for TonB were performed using the Multiseq plug-in for VMD (41). Electrostatic potential maps were calculated using APBS (42) on the equilibrated ( $10 \text{ ns}$ ) structure with a grid spacing of  $<1 \text{ \AA}^3$  per point, protein dielectric constant of  $1.0$ , solvent dielectric constant of  $78.54$ , and mobile ions present at a concentration of  $150 \text{ mM}$ .

## RESULTS AND DISCUSSION

### Association of TonB and BtuB

SMD simulations of the complex began from an equilibrated state (see Methods). The N-terminus of TonB (initially, Pro<sup>153</sup>) was pulled away from BtuB toward the CM, where TonB is at least initially anchored. To assure that the observed behavior is reproducible and independent of the pulling speed, three simulations at pulling speeds of  $10$ ,  $5$ , and  $2.5 \text{ \AA/ns}$ , respectively, were performed. Specific results described below are based on the  $2.5 \text{ \AA/ns}$  simulation except where noted, although similar behaviors were observed and all major events were essentially reproduced in all three simulations (minor differences, though not affecting the main conclusions, are described in Supplementary Material).

In the crystal structure (23), the connection between TonB and BtuB consists primarily of two hydrogen-bonded  $\beta$ -strands, one from each protein. The strand from BtuB is composed of residues  $6\text{--}12$ , the Ton-box, known to be necessary for recruiting TonB ( $15\text{--}17$ ). A conserved salt bridge (between Arg<sup>158</sup> of TonB and Asp<sup>6</sup> of BtuB; Fig. 2) is also observed between TonB and the Ton-box of BtuB.

When pulling of TonB was initiated, the initial  $10\text{--}15 \text{ \AA}$  of elongation was accommodated through the extension of the mostly unstructured N-terminus of TonB. However, the above-noted salt bridge between TonB and the Ton-box served to prevent any further unfolding of TonB, which then moved as a singular unit. This salt bridge was maintained during the entire simulation with a pulling speed of  $2.5 \text{ \AA/ns}$ , nearly so when pulling  $5 \text{ \AA/ns}$ , but only partially when pulling  $10 \text{ \AA/ns}$ . The stability of this electrostatic interaction despite the extension of the N-terminus of TonB supports the suggestion that it may be a nucleation point for binding between TonB and BtuB (23).

Other charge-charge interactions were also observed during an extended equilibration ( $10 \text{ ns}$  total) as well as during the early phase of the SMD simulations; some are illustrated in Fig. 3 A. Although a total of  $11$  salt bridges between TonB and BtuB were observed over the course of the equilibration (although not simultaneously), only two could be classified as stable, namely those between Arg<sup>166</sup> of TonB and Glu<sup>423</sup> of BtuB as well as Arg<sup>204</sup> of TonB and Asp<sup>471</sup> of BtuB (the full list is presented in the Supplementary Material). Although there is significant conservation of positive charges

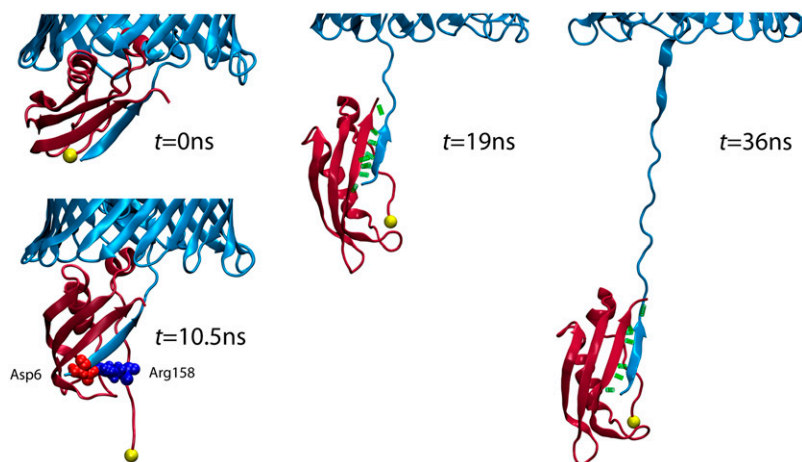


FIGURE 2 Interactions between TonB and the Ton-box of BtuB during unfolding SMD simulations. In all panels, BtuB is shown in light blue and TonB in red and the yellow sphere indicates the pulled atom of TonB. In the second panel ( $t = 10.5$  ns), the conserved salt bridge between Asp<sup>6</sup> of BtuB (red) and Arg<sup>158</sup> (blue) stabilizing the complex is shown in a space-filling representation. In the last two panels ( $t = 19$  ns and  $t = 36$  ns), hydrogen bonds, shown as green rods, serve to maintain the TonB/BtuB connection throughout the entire simulation.

in this area of TonB, neither of residues 423 or 471 in BtuB show noticeable conservation (14). There was also a notable interaction initially present between Arg<sup>212</sup> of TonB and Gln<sup>32</sup> of BtuB. Arg<sup>212</sup> is a well-conserved residue of TonB, whereas Gln<sup>32</sup> is part of the conserved “TEE” motif of TBDTs (14). This interaction presents an interesting contrast

to the structure of FhuA in complex with TonB (24). There, Arg<sup>166</sup> of TonB was observed to interact with Glu<sup>56</sup> of the luminal domain of FhuA (Gln<sup>32</sup> in BtuB) (24). However,  $\sim 25$  extra residues between the Ton-box and the TEE motif in FhuA/TonB allows for this association; in BtuB/TonB, the distance between the two residues is too large (14).

Although no role for individual salt bridges outside of the Ton-box/TonB interaction could be found, an interesting pattern in the distribution of side chains involved in salt bridges between the two proteins was recognized. All residues from BtuB involved in salt bridges were negatively charged (Asp, Glu) and all from TonB were positively charged (Arg, Lys). To see if this pattern could be further generalized, we calculated the electrostatic surface potential maps for both BtuB and TonB at the end of equilibration, shown in Fig. 3, B and C. The two corresponding surfaces shown illustrate that TonB has large regions of positive potential at the surface whereas much of the periplasmic side of BtuB has a negative potential. The complementary electrostatic potentials are suggestive of a means of long-range interaction between TonB and the transporter preceding binding of the two proteins. This suggestion correlates well with the observation that substrate binding increases the negative potential of the region of the luminal domain near the Ton-box (14). Also, the  $\beta$ -strand recruitment of the BtuB Ton-box by TonB (23) pulls this amino-terminal portion of BtuB away from its “folded-in” location in the absence of TonB (9), which changes the electrostatic surface from those previously calculated (14).

During the continued unfolding simulations, extension of the luminal domain of BtuB was seen while the TonB/BtuB interaction remained intact. The arrangement of the  $\beta$ -strands between TonB and BtuB was one source of stability during the mechanical pulling, a hypothesis made previously (23). In the two slowest simulations, the Ton-box/TonB  $\beta$ -strands were oriented vertically relative to the plane of the membrane (and consequently, parallel to the pulling direction). This arrangement affords the connection great stability, requiring shearing all the hydrogen bonds simultaneously to break

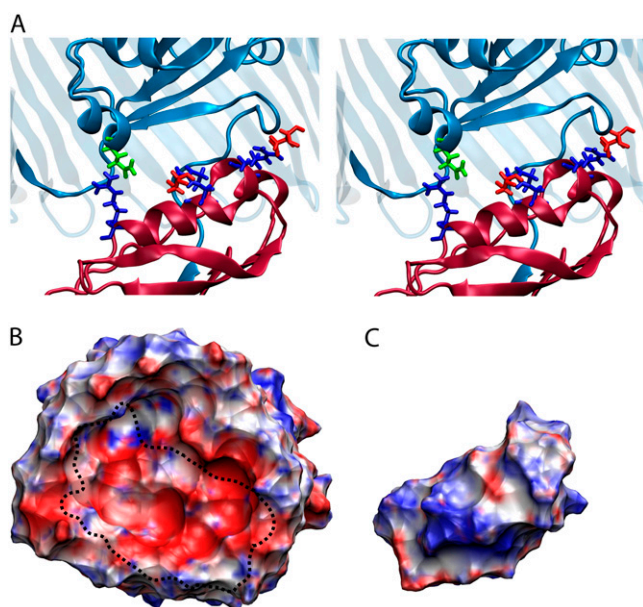


FIGURE 3 Electrostatic interaction between BtuB and TonB. Shown are different views of BtuB and TonB at the end of the 10-ns equilibration. (A) Stereo view of specific salt bridges noted in the text. The barrel of BtuB is transparent and the front half is cut away; TonB and BtuB are colored the same as in Fig. 2. Residues are colored according to type (blue for positive, red for negative, green for polar). The left-most residues are Arg<sup>212</sup> of TonB and Gln<sup>32</sup> of BtuB, the middle ones are Arg<sup>204</sup> of TonB and Asp<sup>471</sup> of BtuB, and on the right are residues Arg<sup>166</sup> of TonB and Glu<sup>423</sup> of BtuB. (B and C) Electrostatic surface potential of BtuB and TonB. Shown are complementary surfaces of (B) the periplasmic face of BtuB with residues 1–20 removed for clarity and (C) the BtuB-facing side of TonB. The potential on the surface is colored from  $-5$  kT/e (red) to  $+5$  kT/e (blue). The dotted line in panel B indicates the location of TonB in the combined structure.

it; this is in contrast to pulling perpendicular to the sequence direction, which can be visualized as “unzipping” the  $\beta$ -strands, breaking the hydrogen bonds sequentially (14). The orientation was also enforced in part by the salt bridge between Arg<sup>158</sup> of TonB and Asp<sup>6</sup> of BtuB, noted above. This salt bridge was well preserved during the slowest simulations although it was broken relatively early in the fastest simulation, leading to a different orientation of the Ton-box/TonB connection. Nonetheless, the overall connection between the two proteins was still maintained in all simulations (see Supplementary Material).

Hydrogen bonding patterns were monitored between the two proteins as a means of quantifying the strength of their association. Hydrogen bonds, mainly in the  $\beta$ -strands connecting TonB to the Ton-box, fluctuated about 10–15 and were as low as eight at one point (see Fig. 2). Other non-specific interactions between TonB and BtuB not including the Ton-box were observed early in the simulation; however, these bonds were easily broken as a result of pulling TonB.

### Unfolding of the luminal domain

The luminal domain is comprised approximately of residues 25–135 of BtuB and provides much of the surface of the substrate binding site as well as an impediment to the transfer of other molecules across the outer membrane by occluding the interior of the barrel (9,23,43). The exact mechanism of formation of a pathway for the substrate is currently unknown, although experimental results have hinted at unfolding of the domain as a possible mechanism (44–46). For example, the luminal domain of FepA, another TBDT, is seen to be unfolded when expressed alone, suggesting a stabilizing role for the barrel (44). Also, in experiments on FhuA where disulfide cross links are formed between the luminal domain and the  $\beta$ -barrel, a cross link formed between the “bottom” portion (i.e., closer to the periplasm, specifically residue 27) of the luminal domain and the  $\beta$ -barrel is not functional (45). In contrast, cross links formed ~80 residues C-terminal to this position in the luminal domain (i.e., farther “up” within the barrel and thus putting less restraint on luminal domain unfolding) remain functional (46).

Our simulations provide a detailed view of the effects of pulling TonB on the luminal domain of BtuB, as illustrated in Fig. 4. Initially, the first  $\beta$ -strand of the luminal domain dissociates by breaking hydrogen bonds sequentially (the “unzipping” mechanism), a relatively low-force event. The forces measured during this process ranged from 50 to 350 pN (see Fig. 5; between ~50 and 70 Å extension); although somewhat high by experimental standards (47,48), this value compares quite well with similar simulations of unzipping/unfolding  $\beta$ -sheet structures where forces were often two to three times as large at the same pulling velocities (49,50).

After the first  $\beta$ -strand of the luminal domain has separated, a large number of residues (45 in total), including two short  $\alpha$ -helices, are present before the next strand of the central  $\beta$ -sheet. Unfolding of helices is also known to occur by breaking hydrogen bonds sequentially and thus should not represent a large rise in force on its own (51,52). However, the unfolding of the two small helices in BtuB is accompanied by the breaking of a number of salt bridges and hydrogen bonds connecting the luminal domain to the barrel. For example, at the end of the simulations at pulling speeds of 2.5 and 5 Å/ns, Arg<sup>36</sup> of BtuB is observed to be nearly separated from Asp<sup>508</sup>, correlating with the force peak seen near the end in Fig. 5 (the simulation at 10 Å/ns was carried out further and displayed further separation of these and other salt bridges). Despite partial unfolding of the luminal domain during pulling, the disturbance to the structure remains localized to the portion being extended; only marginal change is seen in the rest of the domain (RMSD = 1.4–2 Å for residues 50–140 of BtuB). In particular, three substrate binding loops in the apical portion of the luminal domain (defined here as residues 57–65, 71–75, and 88–95, respectively) were not greatly affected even though they are located as few as 10 residues from the unfolded section of the luminal domain (RMSD = 2.2 Å) (14,43).

Although at this point continuing the unfolding simulations with TonB would have been very computationally expensive (because the system size would need to be further increased), the extended portion of the luminal domain could be cut (removing TonB as well) and pulling continued in the same system (see Fig. 6). This was performed for the fastest simulation (10 Å/ns) to determine if unfolding would continue

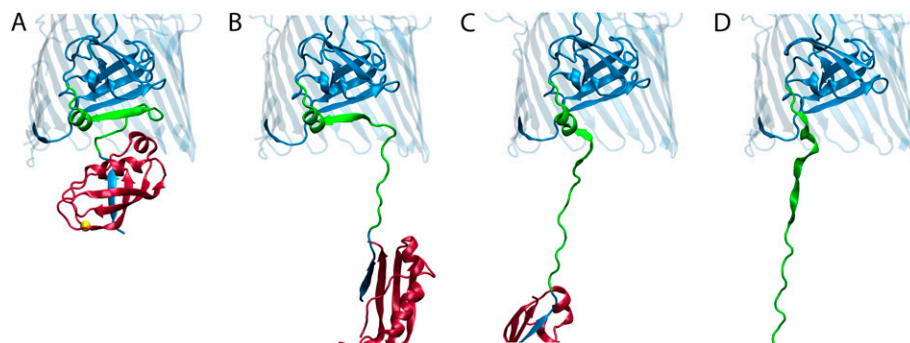


FIGURE 4 Partial unfolding of the “luminal domain”. TonB is shown in red with the N-terminal pulled atom highlighted as a yellow sphere in panel A. The barrel of BtuB is light blue and transparent with the front portion cut away to expose the luminal domain inside. The part of the luminal domain that becomes unfolded during the simulation is shown in green whereas the rest is blue. States of unfolding are shown at approximately (A) 0 Å, (B) 55 Å, (C) 70 Å, and (D) 90 Å of extension.

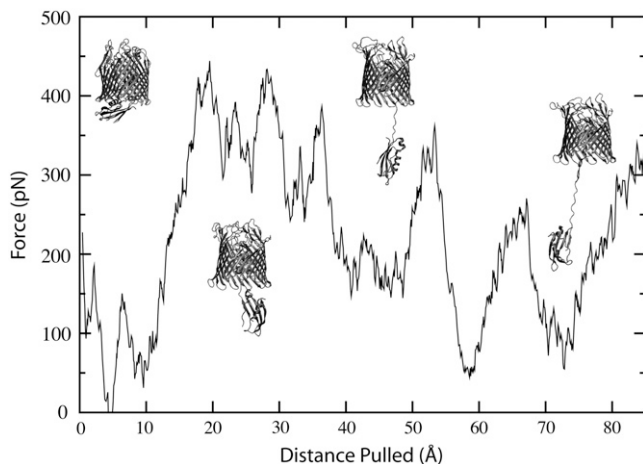


FIGURE 5 Force profile along the TonB pulling direction in unfolding simulations pulling at  $2.5 \text{ \AA/ns}$ . The force applied to the pulled atom is shown as a function of the distance that atom has moved. Insets are of BtuB with TonB at different times in the simulation roughly corresponding to their placement on the plot.

and when transport could occur. It was found that after  $\sim 200 \text{ \AA}$  of total extension, the luminal domain was sufficiently unfolded such that permeation of cyanocobalamin could be accommodated, as shown in Fig. 6 *B*. As the periplasmic width in *E. coli* is  $\sim 180\text{--}235 \text{ \AA}$  (53), such an extension is not impossible. However it is unlikely that such a large extension of the luminal domain will be necessary for the activation. For example, the unfolding of some structures, such as two small helices within the luminal domain, may be an artifact due to the speed of simulation. Thus, we expect actually less extension would be required to reach the same state in vivo.

“Bridging” interfacial water molecules, those that hydrogen bond with both the luminal domain and the barrel of BtuB, were also studied during the course of the unfolding simulations. The number of water molecules bridging the two domains ( $\sim 25$ ) does not change appreciably during the simulation, and matches nearly exactly previous analysis based upon the crystal structure of BtuB (without bound TonB) (14). However, many of the bonds are nonetheless transient, with the specific water molecules forming them changing often, in agreement with previous simulations (22). Thus the water molecules likely serve as a lubricant between the luminal domain and the barrel, mediating the breaking of salt bridges and hydrogen bonds (22). Notably, the space vacated by the luminal domain during further unfolding is easily filled with water during the simulations.

### Unplugging of the luminal domain

In addition to unfolding of the luminal domain, another possible mechanism for exposure of a substrate transport pathway is “unplugging” where the luminal domain leaves

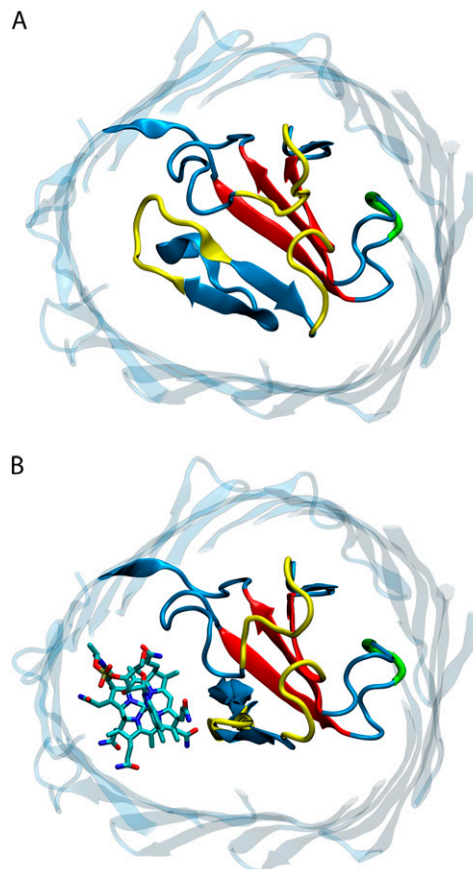


FIGURE 6 Continued unfolding of the luminal domain shown from the extracellular side of the transporter. The barrel of BtuB is light blue and transparent, with extracellular loops removed for clarity. The core  $\beta$ -sheet is shown in red, the substrate binding loops in yellow, the “latch” domain in green, and the remaining portion of the luminal domain in blue. The states shown are snapshots at approximately (A)  $150 \text{ \AA}$  of pulling and (B)  $215 \text{ \AA}$  of pulling. In panel B, cyanocobalamin is placed to scale in the open space created in the transporter.

the barrel as a singular unit without significant conformational change. Although our simulations indicate that unfolding is the natural response of the luminal domain to force applied at the N-terminus, we decided to also investigate the unplugging mechanism through an alternative means of applying force to the transporter. To this end, we removed TonB from our equilibrated system and carried out an SMD simulation where force was applied directly to the center of mass of the luminal domain, attempting to enforce a constant velocity of  $2.5 \text{ \AA/ns}$ , identical to that of the slowest unfolding simulations (see Methods).

The luminal domain in the unplugging simulation proved very reluctant to move, requiring a buildup of  $\sim 4500 \text{ pN}$  before it could be dislodged. At the start of the simulation, 11 salt bridges between the barrel and the luminal domain were present, although 23 in total (not coexisting) were observed forming and breaking at various times during the removal process. The connection between the two domains is also

stabilized initially by  $\sim 60$ – $70$  hydrogen bonds. To forcefully dislodge the luminal domain, a large fraction of the hydrogen bonds and salt bridges must be distressed or broken simultaneously. The force profile, shown in Fig. 7 A, bears out the difficulty of unplugging; at its peak, it requires 10 times the maximum force for unfolding to unplug the luminal domain from the center of the barrel at the same pulling speed. Although this force would be reduced on a longer timescale through the mitigating effect of interfacial waters noted previously, the same effect is expected for unfolding, which disturbs the connection between the luminal domain and the barrel sequentially instead of concurrently.

The difference between the two methods of opening the transporter, unfolding and unplugging, is also illustrated by the behavior of the luminal domain substrate binding loops. In the unfolding simulation pulling at  $2.5 \text{ \AA/ns}$ , the RMSD of the substrate binding loops was at most  $2.2 \text{ \AA}$  near the end of simulation, even when unfolding of the luminal domain had almost reached the first loop. In contrast to this minimal deviation, unplugging the luminal domain from the barrel at the same speed greatly disturbed the substrate binding loops which exhibited an RMSD of  $7 \text{ \AA}$ , even before the luminal domain had left the barrel (and thus would not have yet exposed the substrate to the periplasm). While the luminal domain, including the core  $\beta$ -sheet appears in Fig. 7 B to be relatively intact at the end of the simulation, its RMSD is nearly  $6 \text{ \AA}$  (see supplemental Fig. S9, Supplementary Material).

Recent experiments on the ferric enterobactin transporter FepA provide compelling evidence for a significant change in position of the luminal domain during the transport cycle (54). In the crystal structure of FepA, Gly<sup>54</sup> is located on a surface of the luminal domain that is proximal to the inner surface of the  $\beta$ -barrel. When active transport is abrogated, Gly<sup>54</sup>Cys is not labeled by a small thiol-reactive reagent present in the extracellular and in the periplasmic space (as predicted by the crystal structure). However, during transport, the residue is labeled, accordant with its becoming accessible to the periplasm. This accessibility does not distinguish between unfolding of the luminal domain or unplugging of it (or some combination of the two). However, based on our comparisons of simulated unfolding and unplugging, the application of force through TonB to BtuB seems significantly more likely to result in unfolding of the luminal domain rather than dislodging without significant conformational change.

## CONCLUSION

Employing steered molecular dynamics simulations on a membrane-embedded model of the TonB-BtuB complex, we have examined a functional hypothesis based on the structures of both TonB and TBBDTs, and of the two in complex (14,23,24), and have presented an initial view of the dynamics and mechanical properties of a key molecular link between the cytoplasmic and outer membranes of Gram-negative bacteria. The durability of the coupling between TonB and BtuB seen in this study demonstrates that TonB is capable of transmitting force to proteins embedded in the outer membrane through a small, yet strong contact region; given that different orientations of TonB were observed in the simulations, the strength of coupling may be relatively independent of pulling direction. Also, the C-terminal domain of TonB proved to be able to withstand such forces without significant distortion of its own structure (see supplemental Fig. S6-A, Supplementary Material). Taken together, these data support the feasibility of a mechanical mode of energy transduction reaching across the periplasm as the means of import of large molecules. Our calculations, however, do not examine and thus cannot exclude the possibility of alternative activation mechanisms, e.g., the shuttle model (28,29). Regardless of the mechanism utilized, the formation of the complex appears to be influenced by a long-range electrostatic attraction, mediated by a large number of oppositely charged residues on TonB and the transporter.

Our results have also tentatively resolved a key step in the activation mechanism, namely the initial conformational response of the luminal domain to mechanical stress, which triggers the transport of the substrate through the  $\beta$ -barrel domain. Experiments have strongly indicated that the

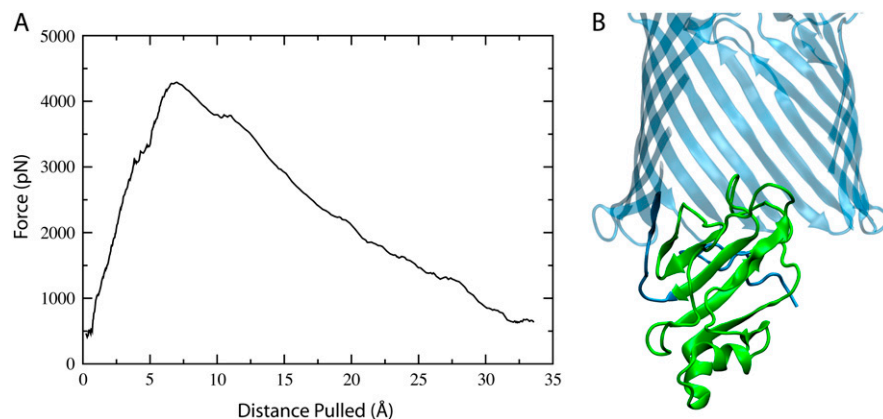


FIGURE 7 Unplugging of the luminal domain. (A) Force profile along the pulling direction. The force applied to the center-of-mass of the luminal domain is shown as a function of the distance pulled. (B) Final state of BtuB after 14 ns. The barrel of BtuB is shown transparent in light blue with the front portion cut away. The luminal domain is colored mostly green, representing the residues included for pulling the center of mass, whereas blue represents those not pulled.

luminal domain at least partially leaves the barrel during substrate transport, suggesting either unfolding of the luminal domain or an unplugging motion where the luminal domain leaves the barrel reasonably intact (54). Assuming a mechanical coupling between TonB and the transporter, our simulations indicate the former (unfolding) is much more likely, requiring one-tenth the force as compared to pulling the luminal domain out intact at the same speed. However, additional experimental and computational studies are certainly required to develop a more detailed image of what combinations of rigid body movement, conformational change, and unfolding may actually occur in vivo within the cell. For instance, slight unfolding through the action of TonB might be sufficient to trigger spontaneous additional unfolding or other conformational changes that expose a permeation pathway. The induced partial unfolding of the luminal domain in our simulations does not greatly disturb the extracellular substrate binding loops until a permeation pathway becomes exposed, at which point such a disturbance could cause cyanocobalamin, which normally is bound with nanomolar affinity, to be released. Transient interfacial water molecules were also observed and likely play a role in facilitating the separation of the luminal domain from the barrel.

These conclusions, applicable to all TonB-dependent transporters, encourage further computation and experimentation examining both the resistance of TonB to unfolding as well as the propensity of the luminal domain to unfold under mechanical stress. Additional simulations will further investigate the mechanistic details of selectivity as well as a recently discovered signal transduction pathway that underlies the allosteric mechanism in TBDTs (55).

## SUPPLEMENTARY MATERIAL

To view all of the supplemental files associated with this article, visit [www.biophysj.org](http://www.biophysj.org).

The authors gratefully acknowledge computer time provided by the Pittsburgh Supercomputing Center, the National Center for Supercomputing Applications, and Indiana University through the National Resources Allocation Committee (MCA93S028 and MCA06N060).

This work was supported by the National Institutes of Health (P41-RR05969, R01-GM067887 for J.G. and E.T., and R01-DK59999 for M.C.W.).

## REFERENCES

- Nikaido, H. 1994. Porins and specific diffusion channels in bacterial outer membranes. *J. Biol. Chem.* 269:3905–3908.
- Nikaido, H. 1994. Prevention of drug access to bacterial targets—permeability barriers and active efflux. *Science*. 264:382–388.
- Postle, K., and R. J. Kadner. 2003. Touch and go: tying TonB to transport. *Mol. Microbiol.* 49:869–882.
- Ferguson, A. D., E. Hofmann, J. W. Coulton, K. Diederichs, and W. Welte. 1998. Siderophore-mediated iron transport: crystal structure of FhuA with bound lipopolysaccharide. *Science*. 282:2215–2220.
- Locher, K. P., B. Rees, R. Koebnik, A. Mitschler, L. Moulinier, J. P. Rosenbusch, and D. Moras. 1998. Transmembrane signaling across the ligand-gated FhuA receptor: crystal structures of free and ferrichrome-bound states reveal allosteric changes. *Cell*. 95:771–778.
- Buchanan, S. K., B. S. Smith, L. Venkatramani, D. Xia, L. Esser, M. Palnitkar, R. Chakraborty, D. van der Helm, and J. Deisenhofer. 1999. Crystal structure of the outer membrane active transporter FepA from *Escherichia coli*. *Nat. Struct. Biol.* 6:56–63.
- Ferguson, A. D., R. Chakraborty, B. S. Smith, L. Esser, D. van der Helm, and J. Deisenhofer. 2002. Structural basis of gating by the outer membrane transporter FecA. *Science*. 295:1715–1719.
- Yue, W. W., S. Grizot, and S. K. Buchanan. 2003. Structural evidence for iron-free citrate and ferric citrate binding to the TonB-dependent outer membrane transporter FecA. *J. Mol. Biol.* 332:353–368.
- Chimento, D. P., A. K. Mohanty, R. J. Kadner, and M. C. Wiener. 2003. Substrate-induced transmembrane signaling in the cobalamin transporter BtuB. *Nat. Struct. Biol.* 10:394–401.
- Cobessi, D., H. Celia, N. Folschweiller, I. J. Schalk, M. A. Abdallah, and F. Pattus. 2005. The crystal structure of the pyoverdine outer membrane receptor FpvA from *Pseudomonas aeruginosa* at 3.6 Å resolution. *J. Mol. Biol.* 347:121–134.
- Cobessi, D., H. Celia, and F. Pattus. 2005. Crystal structure at high resolution of ferric-pyochelin and its membrane receptor FptA from *Pseudomonas aeruginosa*. *J. Mol. Biol.* 352:893–904.
- Klebba, P. E. 2003. Three paradoxes of ferric enterobactin uptake. *Front. Biosci.* 8:S1422–S1436.
- Wiener, M. C. 2005. TonB-dependent outer membrane transport: going for Baroque? *Curr. Opin. Struct. Biol.* 15:394–400.
- Chimento, D. P., R. J. Kadner, and M. C. Wiener. 2005. Comparative structural analysis of TonB-dependent outer membrane transporters: implications for the transport cycle. *Proteins*. 59:240–251.
- Kadner, R. J. 1990. Vitamin B12 transport in *Escherichia coli*: energy coupling between membranes. *Mol. Microbiol.* 4:2027–2033.
- Lundrigan, M. D., and R. J. Kadner. 1986. Nucleotide sequence of the gene for the ferrienterochelin receptor FepA in *Escherichia coli*. Homology among outer membrane receptors that interact with TonB. *J. Biol. Chem.* 261:10797–10801.
- Schramm, E., J. Mende, V. Braun, and R. M. Kamp. 1987. Nucleotide sequence of the colicin B activity gene *cba*: consensus pentapeptide among TonB-dependent colicins and receptors. *J. Bacteriol.* 169:3350–3357.
- Cadieux, N., and R. J. Kadner. 1999. Site-directed disulfide bonding reveals an interaction site between energy-coupling protein TonB and BtuB, the outer membrane cobalamin transporter. *Proc. Natl. Acad. Sci. USA*. 96:10673–10678.
- Cadieux, N., C. Bradbeer, and R. J. Kadner. 2000. Sequence changes in the ton box region of BtuB affect its transport activities and interaction with TonB protein. *J. Bacteriol.* 182:5954–5961.
- Merianos, H. J., N. Cadieux, C. H. Lin, R. J. Kadner, and D. S. Cafiso. 2000. Substrate-induced exposure of an energy-coupling motif of a membrane transporter. *Nat. Struct. Biol.* 7:205–209.
- Ferguson, A. D., and J. Deisenhofer. 2004. Metal import through microbial membranes. *Cell*. 116:15–24.
- Faraldo-Gómez, J. D., G. R. Smith, and M. S. P. Sansom. 2004. Molecular dynamics simulations of the bacterial outer membrane protein FhuA: a comparative study of the ferrichrome-free and bound states. *Biophys. J.* 85:1406–1420.
- Shultz, D. D., M. D. Purdy, C. N. Banchs, and M. C. Wiener. 2006. Outer membrane active transport: structure of the BtuB:TonB complex. *Science*. 312:1396–1399.
- Pawelek, P. D., N. Croteau, C. Ng-Thow-Hing, C. M. Khursigara, N. Moiseeva, M. Allaire, and J. W. Coulton. 2006. Structure of TonB in complex with FhuA, *E. coli* outer membrane receptor. *Science*. 312:1399–1402.
- Chang, C., A. Mooser, A. Pluckthun, and A. Wlodawer. 2001. Crystal structure of the dimeric C-terminal domain of TonB reveals a novel fold. *J. Biol. Chem.* 276:27535–27540.
- Ködding, J., F. Killig, P. Polzer, S. P. Howard, K. Diederichs, and W. Welte. 2005. Crystal structure of a 92-residue C-terminal fragment



- of TonB from *Escherichia coli* reveals significant conformational changes compared to structures of smaller TonB fragments. *J. Biol. Chem.* 280:3022–3028.
27. Peacock, R. S., A. M. Weljie, S. P. Howard, F. D. Price, and H. J. Vogel. 2005. The solution structure of the C-terminal domain of TonB and interaction studies with TonB box peptides. *J. Mol. Biol.* 345: 1185–1197.
  28. Letain, T. E., and K. Postle. 1997. TonB protein appears to transduce energy by shuttling between the cytoplasmic membrane and the outer membrane in Gram-negative bacteria. *Mol. Microbiol.* 24:271–283.
  29. Larsen, R. A., and K. Postle. 2003. *In vivo* evidence of TonB shuttling between the cytoplasmic and outer membrane in *Escherichia coli*. *J. Bacteriol.* 145:211–218.
  30. Brockwell, D. J., E. Paci, R. C. Zinober, G. S. Beddard, P. D. Olmsted, D. A. Smith, R. N. Perham, and S. E. Radford. 2003. Pulling geometry defines the mechanical resistance of a  $\beta$ -sheet protein. *Nat. Struct. Biol.* 10:731–737.
  31. Carrion-Vazquez, M., H. Li, H. Lu, P. Marszalek, A. Oberhauser, and J. Fernandez. 2003. The mechanical stability of ubiquitin is linkage dependent. *Nat. Struct. Biol.* 10:738–743.
  32. Ash, W. L., M. R. Zlomislic, E. O. Oloo, and D. P. Tieleman. 2004. Computer simulations of membrane proteins. *Biochim. Biophys. Acta.* 1666:158–189.
  33. Gumbart, J., Y. Wang, A. Aksimentiev, E. Tajkhorshid, and K. Schulten. 2005. Molecular dynamics simulations of proteins in lipid bilayers. *Curr. Opin. Struct. Biol.* 15:423–431.
  34. Gao, M., M. Sotomayor, E. Villa, E. Lee, and K. Schulten. 2006. Molecular mechanisms of cellular mechanics. *Phys. Chem. Chem. Phys.* 8:3692–3706.
  35. Israilewitz, B., M. Gao, and K. Schulten. 2001. Steered molecular dynamics and mechanical functions of proteins. *Curr. Opin. Struct. Biol.* 11:224–230.
  36. Humphrey, W., A. Dalke, and K. Schulten. 1996. VMD: visual molecular dynamics. *J. Mol. Graph.* 14:33–38.
  37. Phillips, J. C., R. Braun, W. Wang, J. Gumbart, E. Tajkhorshid, E. Villa, C. Chipot, R. D. Skeel, L. Kale, and K. Schulten. 2005. Scalable molecular dynamics with NAMD. *J. Comput. Chem.* 26:1781–1802.
  38. MacKerell, A. D. Jr., D. Bashford, M. Bellott, R. L. Dunbrack Jr., J. Evanseck, M. J. Field, S. Fischer, J. Gao, H. Guo, S. Ha, D. Joseph, L. Kuchnir, et al. 1998. All-atom empirical potential for molecular modeling and dynamics studies of proteins. *J. Phys. Chem. B.* 102: 3586–3616.
  39. Izrailev, S., S. Stepaniants, M. Balsera, Y. Oono, and K. Schulten. 1997. Molecular dynamics study of unbinding of the avidin-biotin complex. *Biophys. J.* 72:1568–1581.
  40. Gumbart, J., and K. Schulten. 2006. Molecular dynamics studies of the archaeal translocon. *Biophys. J.* 90:2356–2367.
  41. Roberts, E., J. Eargle, D. Wright, and Z. Luthey-Schulten. 2006. MultiSeq: unifying sequence and structure data for evolutionary analysis. *BMC Bioinformatics.* 7:382.
  42. Baker, N. A., D. Sept, S. Joseph, M. J. Holst, and J. A. McCammon. 2001. Electrostatics of nanosystems: application to microtubules and the ribosome. *Proc. Natl. Acad. Sci. USA.* 98:10037–10041.
  43. Chimento, D. P., R. J. Kadner, and M. C. Wiener. 2003. The *Escherichia coli* outer membrane cobalamin transporter BtuB: structural analysis of calcium and substrate binding, and identification of orthologous transporters by sequence/structure conservation. *J. Mol. Biol.* 332:999–1014.
  44. Usher, K. C., E. Özkan, K. H. Gardner, and J. Deisenhofer. 2001. The plug domain of FepA, a TonB-dependent transport protein from *Escherichia coli*, binds its siderophore in the absence of the transmembrane barrel domain. *Proc. Natl. Acad. Sci. USA.* 98:10676–10681.
  45. Endriss, F., M. Braun, H. Killmann, and V. Braun. 2003. Mutant analysis of the *Escherichia coli* FhuA protein reveals sites of FhuA activity. *J. Bacteriol.* 185:4683–4692.
  46. Eisenhauer, H. A., S. Shames, P. D. Pawelek, and J. W. Coulton. 2005. Siderophore transport through *Escherichia coli* outer membrane receptor FhuA with disulfide-tethered cork and barrel domains. *J. Biol. Chem.* 280:30574–30580.
  47. Oberhauser, A. F., P. K. Hansma, M. Carrion-Vazquez, and J. M. Fernandez. 2001. Stepwise unfolding of titin under force-clamp atomic force microscopy. *Proc. Natl. Acad. Sci. USA.* 98:468–472.
  48. Li, L. W., H. H. L. Huang, C. L. Badilla, and J. M. Fernandez. 2005. Mechanical unfolding intermediates observed by single-molecule force spectroscopy in a fibronectin type III module. *J. Mol. Biol.* 345: 817–826.
  49. Gao, M., D. Craig, O. Lequin, I. D. Campbell, V. Vogel, and K. Schulten. 2003. Structure and functional significance of mechanically unfolded fibronectin type IIII intermediates. *Proc. Natl. Acad. Sci. USA.* 100:14784–14789.
  50. Lee, E. H., M. Gao, N. Pinotsis, M. Wilmanns, and K. Schulten. 2006. Mechanical strength of the titin Z1Z2/telethonin complex. *Structure.* 14:497–509.
  51. Lu, H., and K. Schulten. 1999. Steered molecular dynamics simulations of force-induced protein domain unfolding. *Proteins.* 35:453–463.
  52. Rohs, R., C. Etchebest, and R. Lavery. 1999. Unraveling proteins: a molecular mechanics study. *Biophys. J.* 76:2760–2768.
  53. Matias, V. R. F., A. Al-Amoudi, J. Dubocher, and T. J. Beveridge. 2003. Cryo-transmission electron microscopy of frozen-hydrated sections of *Escherichia coli* and *Pseudomonas aeruginosa*. *J. Bacteriol.* 185:6112–6118.
  54. Ma, L., W. Kaserer, R. Annamalai, D. C. Scott, B. Jin, X. Jiang, Q. Xiao, H. Maymani, L. M. Massis, L. C. Ferreira, S. M. C. Newton, and P. E. Klebba. 2007. Evidence of ball-and-chain transport of ferric enterobactin through FepA. *J. Biol. Chem.* 282:397–406.
  55. Ferguson, A. D., C. A. Amezcua, N. M. Halabi, Y. Chelliah, M. K. Rosen, R. Ranganathan, and J. Deisenhofer. 2007. Signal transduction pathway of TonB-dependent transporters. *Proc. Natl. Acad. Sci. USA.* 104:513–518.